Technical University of Denmark

DTU

The DAN-AERO MW Experiments
Final report

Aagaard Madsen , Helge; Bak, Christian; Schmidt Paulsen, Uwe; Gaunaa, Mac; Fuglsang, Peter; Romblad, Jonas; Olesen, Niels A.; Enevoldsen, Peder; Laursen, Jesper; Jensen, Leo

Link back to DTU Orbit

DTU Library
Technical Information Center of Denmark

The DAN-AERO MW Experiments
Final report

Helge Aagaard Madsen, Christian Bak, Uwe Schmidt Paulsen
and Mac Gaunaa (Risø DTU), Peter Fuglsang (LM Glasfiber),
Jonas Romblad and Niels A. Olesen (Vestas Wind Systems),
Peder Enevoldsen and Jesper Laursen (Siemens Wind Power),
Leo Jensen (DONG Energy)

Risø-R-1726(EN)
September 2010

Risø DTU
National Laboratory for Sustainable Energy

Author: Helge Aagaard Madsen, Christian Bak, Uwe Schmidt Paulsen and Mac Gaunaa (Risø DTU), Peter Fuglsang (LM Glasfiber), Jonas Romblad and Niels A. Olesen (Vestas Wind Systems), Peder Enevoldsen and Jesper Laursen (Siemens Wind Power), Leo Jensen (DONG Energy)

Abstract (max. 2000 char.):

This report describes the DAN-AERO MW experiments carried out within a collaborative, three years research project between Risø DTU and the industrial partners LM Glasfiber, Siemens Wind Power, Vestas Wind Systems A/S and the utility company DONG Energy. The main objective of the project was to establish an experimental data base which can provide new insight into a number of fundamental aerodynamic and aero-acoustic issues, important for the design and operation of MW size turbines. The most important issue is the difference between airfoil characteristics measured under 2D, steady conditions in a wind tunnel and the unsteady 3D flow conditions on a rotor. The different transition characteristics might explain some of the differences between the 2D and 3D airfoil data and the experiments have been set up to provide data on this subject. The overall experimental approach has been to carry out a number of coordinated, innovative measurements on full scale MW size rotors as well as on airfoils for MW size turbines in wind tunnels. Shear and turbulence inflow characteristics were measured on a Siemens 3.6 MW turbine with a five hole pitot tube. Pressure and turbulent inflow characteristics were measured on a 2MW NM80 turbine with an 80 m rotor. One of the LM38.8 m blades on the rotor was replaced with a new LM38.8 m blade where instruments for surface pressure measurements at four radial sections were build into the blade during the blade production process. Additionally, the outmost section on the blade was further instrumented with around 50 microphones for high frequency surface pressure measurements. The surface pressure measurements have been correlated with inflow measurements from four five hole pitot tubes and two sensors for measuring the high frequency (50 Hz to10 kHz) contents of the inflow turbulence. In parallel, 2D wind tunnel measurements on common airfoils for wind turbine applications have been conducted in three different wind tunnels at Delft University (NL), at LM Glasfiber (DK) and at VELUX (DK). Initial results from the different measurement set-ups are presented in order to show the application areas for the total data set.

Contents

Preface

The present report is the final publishable report for the project "Experimental Rotor- and Airfoil Aerodynamics on MW Wind Turbines", also called the DAN-AERO MW project, funded by the Danish Energy Research programme EFP-2007 under contract Journal nr.: 33033-0074. The project was carried out in the period from March 2007 to December 2009 in corporation between Risø DTU and the companies LM Glasfiber, Vestas Wind Systems, Siemens Wind Power and DONG Energy.

The project comprised a number of innovative and coordinated measurements on full scale turbines and measurements in wind tunnels on airfoil sections. This was only possible due to a close and fruitful corporation between technicians and engineers from all involved partners in the project and we would like to thank all involved persons. Also thank to the companies LM Glasfiber, Vestas Wind Systems A/S, Siemens Wind Power and DONG Energy for the considerable eigen funding contribution to the project.

The result of the project is a considerable and unique data base, which contains data that research projects during the next years will benefit from. A detailed analysis of the data is not contained in the present project. This will be performed in a new project "DANAERO MW II: Influence of atmospheric and wake turbulence on MW turbine performance, loading and stability" funded by the Danish Energy Research Programme EUDP with the participants Risoe DTU, LM Glasfiber, Vestas Wind Systems A/S and Siemens Wind Power.

The objective with the present report is to give a short overview of the different experiments carried out within the project and give an introduction to the data base by showing different examples of data. However, it should be noted that most data that will be shown are derived with preliminary calibrations of the sensors.

Helge Aagaard Madsen and Christian Bak

Risø DTU, March 2010

1 Introduction

The background for the present project initiated in 2007 was a discussion and assessment in the project group of the uncertainties and shortcomings related to the reliable design of MW turbines. The most important issue is that the derivation of 3D airfoil data from 2D wind tunnel data still introduces uncertainty and conservatism in the rotor design process although different empirical correction methods have been developed. It is now also possible to extract 3D data from full 3D CFD rotor computations [1], but these complex simulations need further validation. One major uncertainty related to the 3D CFD rotor computations is that these types of simulations so far have been restricted to non-turbulent, steady inflow conditions. Also the transition modelling is subject to considerable uncertainty and in particular in 3D flow cases. Therefore, measured 3D airfoil characteristics on a MW rotor in natural, turbulent flow environment are needed to be compared with standard 2D wind tunnel data. This will improve the 2D to 3D conversion of airfoil data and also represent a unique verification basis for 3D CFD computations.

Another fundamental issue is related to the aerodynamic load variations over the swept area of MW rotors, which now have reached a size with a rotor diameter of 100 m or more. These load variations, which are due to wind shear and turbulence cause considerable dynamic variation in induction over the rotor and the modeling of this with the Blade Element Momentum (BEM) method is uncertain. Generally, there is a need for detailed characterization of the inflow characteristics on MW rotors and not least to get experimental data for the higher frequencies in the inflow which are thought to be important for the transition from laminar to turbulent boundary layer on the rotating blade.

The new MW rotors are almost exclusively erected in wind farms which means that operation in wakes from upstream turbines constitutes a major part of total life time. Detailed measurements of flow characteristics in full scale wakes are sparse, but on the other hand strongly needed for further improvements of wake modeling.

In the past the aerodynamics of wind turbine rotors operating in real wind conditions have also been recognized to be of big importance for reliable design of turbines. In the period from around 1985 to 1995 this led to a number of field test measurements on rotors with a diameter in the range from 10-25 m conducted at National Renewable Energy Laboratory (NREL, US), Risø Wind Turbine Test Station (Risø, DK), Netherlands Energy Research Foundation (ECN, NL), Delft University of Technology (Delft, NL), Imperial College (IC, UK) and MIE University (MIE, JP). The Risø experiment [2] comprised measurements of local aerodynamic forces at three stations on one of the blades on the 19 m rotor and correlation with inflow measurements with a five hole pitot tube. The derived 3D airfoil characteristics were found to differ considerably from 2D wind tunnel characteristics.

A collaborative and coordinated analysis of the different field rotor experiments was carried out within the IEA Annexes XIV and XVIII, which improved the insight into 3D airfoil characteristics on rotors considerably. However, it was also realized that the influence of the natural turbulence in the wind complicated the interpretation of the results. To overcome this NREL in US conducted the Unsteady Aerodynamics

Experiment (UAE) on a 10 m diameter horizontal axis wind turbine (HAWT) in the NASA Ames 80 ft by 120 ft (24.4 m by 36.6 m) wind tunnel in year 2000 [3]. The experiment was designed to provide accurate and reliable experimental measurements, having high spatial and temporal resolution, for realistic rotating blade geometry, under closely matched conditions of dynamic similarity, and in the presence of strictly controlled inflow conditions. Also these data were analyzed and utilized for code development and validation within IEA Annex XX. Later in 2006 a European team conducted a complementary wind tunnel turbine test designated MEXICO (Model Rotor Experiments In Controlled Conditions) [4]. The MEXICO Project was directed toward acquiring high quality experimental data, by testing a well instrumented 4.5m diameter rotor in the DNW 9.5 m x 9.5 m wind tunnel. This experiment comprised among other measurements comprehensive measurements of the flow field around the rotor using the PIV technique. Also this data set is now utilized in a collaborative work within IEA Task 29 MEXNEXT.

The above mentioned data sets from wind tunnel experiments in controlled wind conditions have contributed significantly to model development and validation and not least for validation of CFD rotor computations. On the other hand there are some serious limitations when the the knowledge is transferred to full scale MW rotors. The most important is the lack of the influence from the unsteady and turbulent inflow, which in the end has to be taken into account although it complicates detailed aerodynamic measurements as well as simulations. Another major drawback of the wind tunnel data sets is that the rotors are not representative for modern MW rotor designs and do not contain the influence of the control system. Finally, there is the unavoidable uncertainty from the much lower Reynolds number in the wind tunnel experiments compared with full-scale conditions.

These considerations led to the decision in the present project group that it was time to initiate a comprehensive experimental project: the DAN-AERO MW Experiments, focusing on fundamental aerodynamics and aeroacoustics issues of MW turbines. The project was initiated in the beginning of 2007 and ended on December 31 2009. However, the detailed analysis of the data is not included in the present project but will be carried out in a new project "The DAN_AERO MW II project" initiated on March 1st 2010 and with the same project participants as in the present project except that DONG Energy is not participating in the new project.

2 Objectives and approach

2.1 Objectives

The overall objective of the project has been to provide an experimental basis that can improve our knowledge of a number of fundamental aerodynamic, aeroelastic and aeroacoustic issues and in general improve the design basis for MW rotors. Specifically the experiments were designed to provide new insight into:

- correlation between 2D and 3D airfoil characteristics

- boundary layer transition characteristics in 2D wind tunnel flow environment compared with full scale 3D rotor flow transition characteristics

- inflow characteristics (shear and turbulence) on MW rotors with particular focus on the high frequency content

- dynamic induction characteristics

- wake flow characteristics

- pressure fluctuations in the boundary layer influencing turbulent inflow noise and trailing edge noise

2.2 Approach

The selected experimental approach has been to carry out a number of coordinated, innovative measurements on full scale MW rotors as well as on airfoils for MW turbines in wind tunnels. Three types of measurements have been performed:

1. Measurements on 2D airfoil sections in three wind tunnels; at Delft University (NL), at LM Glasfiber (DK) and at Velux (DK)

2. Measurement of inflow characteristics on the 3.6 MW Siemens wind turbine at the Høvsøre test site (DK)

3. Pressure and inflow measurements (including high frequency kHz data) on one of the blades (LM 38.8 m blade) on the NM80 2 MW turbine at the small Tjæreborg Wind farm in Jutland (DK)

Wind tunnel experiments

The specific objectives with the wind tunnel experiments were the following:

a) verify and investigate the difference in 2D airfoil characteristics measured in three different wind tunnels: at Delft University (NL), at LM Glasfiber (DK) and at Velux (DK), which in the past have been used for testing airfoils for wind turbines

b) investigate the turbulence characteristics in the wind tunnels and investigate the correlation with boundary layer transition and surface pressure spectra

c) measure the 2D airfoil characteristics on the four specific sections on the LM 38.8 m blade for comparison with 3D airfoil characteristics of the NM80 rotor.

One problem often encountered in the design of a new wind turbine rotor is that the airfoil data from different wind tunnels deviate. It was therefore decided to include the test of two airfoils, the Risø-B1-18 and the NACA 63_3-418 airfoil, in the three wind

tunnels mentioned above. The turbulence characteristics in the tunnels are an important parameter with influence on the transition characteristics on the airfoils and measurements with hotwires have been performed to determine the turbulence spectra in two of the tunnels.

Position of transition has been determined by analyzing the PSD spectra of the high frequency surface pressure fluctuations measured with microphones mounted close to the blade surface, Figure 1. In total around 80 microphones were positioned around the

Figure 1 Microphones with a diameter of around 4 mm installed about 1 mm below the blade section surface and connected through a boring of 1.5 mm.
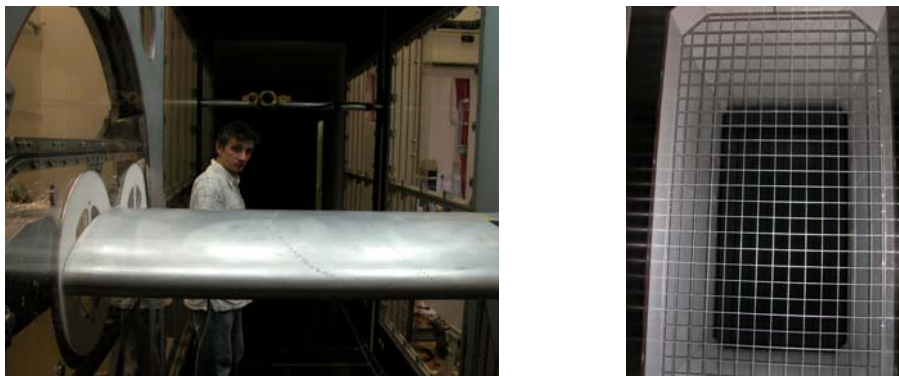
Figure 2 To the left one of the airfoil sections with pressure taps and microphones mounted in the LM wind tunnel. To the right a view into the inlet to the test section with a turbulence grid installed.

surface of the airfoil section at one spanwise position, both on the pressure and suction side. However, the microphone positions were shifted slightly in spanwise direction in order to avoid disturbance from one microphone to the next. The tests performed in the LM wind tunnel, Figure 2 were carried out at a number of different Reynolds numbers from 1.6 million to 6 million. Influence of increased turbulence from a turbulence grid in the inlet to the test section in the LM wind tunnel was also measured, Figure 2.

Inflow measurements on the Siemens 3.6 MW turbine

The increase in wind turbine rotor size with rotor diameters up to above 120 m has led to bigger variations of inflow characteristics over the rotor plane. Considerable wind shear gives higher rotor moments and influences the aerodynamic performance of the turbine. It also complicates the measurement of rotor performance as the standard so far has been to use a hub height cup anemometer some distance upstream the turbine which does not

necessarily result in a wind speed that is a good measure of the average wind speed over the rotor area. There is thus a need for detailed information of inflow characteristics (shear as well as turbulence characteristics) over the rotor plane. The standard technique for obtaining such information has for a long time been a meteorology mast with a suitable instrumentation of anemometers, wind direction vanes and sonics. Within the last few years sodar and lidar techniques have been introduced and this seems to be promising techniques although still expensive [5].

In the past we have investigated an approach which is based on the measurement of the inflow on the rotating blade of a rotor. So far a five hole pitot tube is used, which gives the magnitude of the flow velocity and two flow angles. The main advantages with this measurement technique are; 1) the flow sensor scans along a circular path on the swept rotor area; 2) the measurement is performed at exactly the position of the operating rotor and 3) the instrumentation is relatively cheap. The main disadvantage is that the measured data have to be corrected for the influence of the rotor forces if it shall correspond to free inflow conditions.

In the present project wind shear and turbulence data have been investigated on basis of inflow measurements on the Siemens 3.6 MW turbine at the Høvsøre Test site for MW turbines, Jutland (DK). In March 2007 a five hole pitot tube was installed at a radius of 36 m on the 107 m diameter rotor, Figure 3, for measurement of local inflow angle and relative velocity. This position corresponds to r/R=0.673. The Høvsøre test site is the Danish centre for testing MW turbines and is situated a few kilometres from the west cost of Jutland. In total five turbines are installed along a row at the test site and the Siemens turbine is situated in the middle of this row so the turbine will operate in wake of other turbines for some wind directions, Figure 4. The signals from the pitot tube have been sampled at 35 Hz together with a number of signals from the turbine such as electrical power and rotor rotational speed.

Figure 3 The five hole pitot tube mounted in radius 36 m on the blade in a distance of about 0.80 m in front of the leading edge of the blade. Rotor diameter is 107 m.
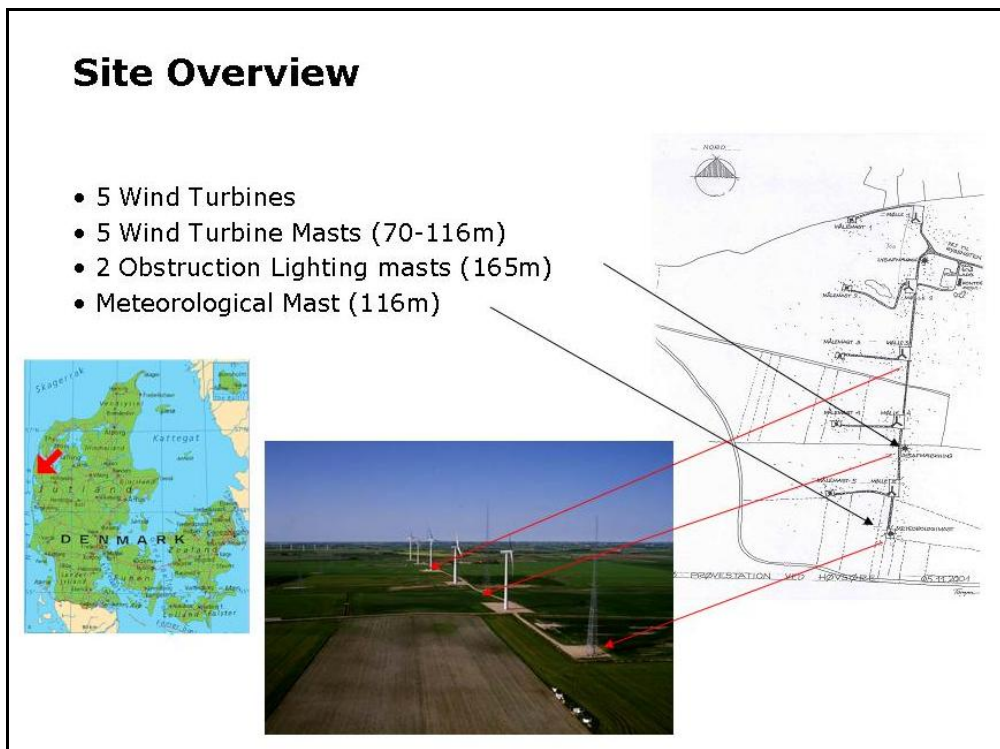
Figure 4 The Høvsøre test site in Jutland. The Siemens 3.6 MW turbine is situated as the middle turbine in the row of 5 turbines.

Inflow and surface pressure measurements on the 2MW NM80 turbine at the Tjæreborg wind farm

The specific objectives with this part of the project have been to:

a) derive and investigate 3D airfoil characteristics from a full scale MW rotor on basis of blade surface pressure measurements at four radial stations in combination with local inflow measurements with five hole pitot tubes at the same radial positions. Compare the 3D airfoil characteristics with 2D wind tunnel data and use the data sets for validation and further development of models for 2D to 3D conversions.

b) investigate the influence of different aerodynamic devices such as vortex generators, gurney flaps and roughness/transition elements on the pressure distributions.

A new LM38.8 m blade was manufactured for the NM80 80m diameter turbine and during the production process, equipment for measuring surface pressure profiles and inflow at four radial stations was placed inside the blade, Figure 5 and Figure 6. Additionally, the most outboard blade section was instrumented with around 50 microphones to measure high frequency surface pressure spectra, Figure 7. These data are used for determination of position of transition and for aeroacoustic characterization of inflow noise and trailing edge noise from the turbulent boundary layer. At a radial position close to the microphones, high frequency inflow has in a few campaigns been measured with a hot wire probe and with a pitot tube with microphones. Local inflow was measured at four radial positions with five hole pitot tubes, Figure 8.
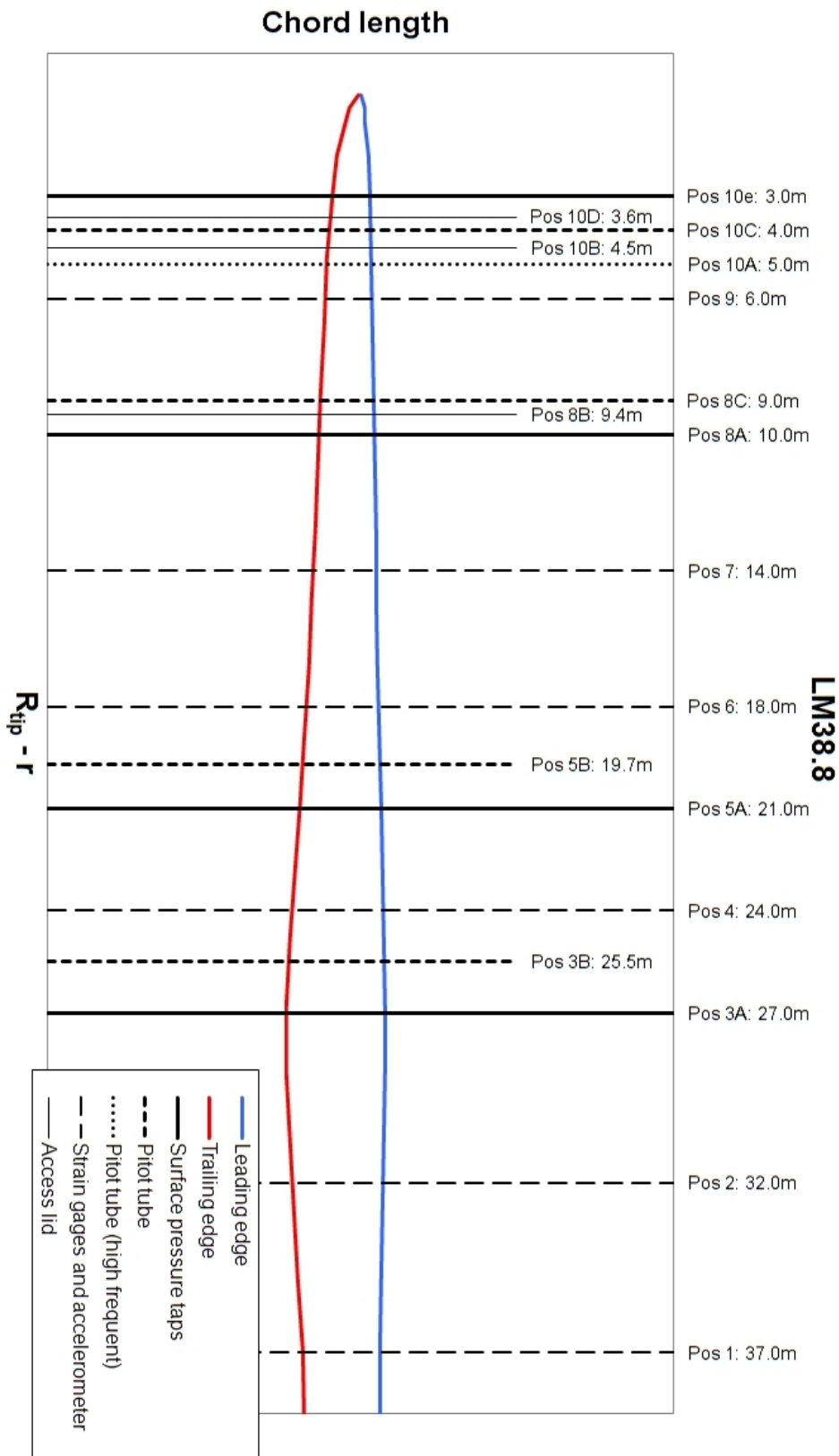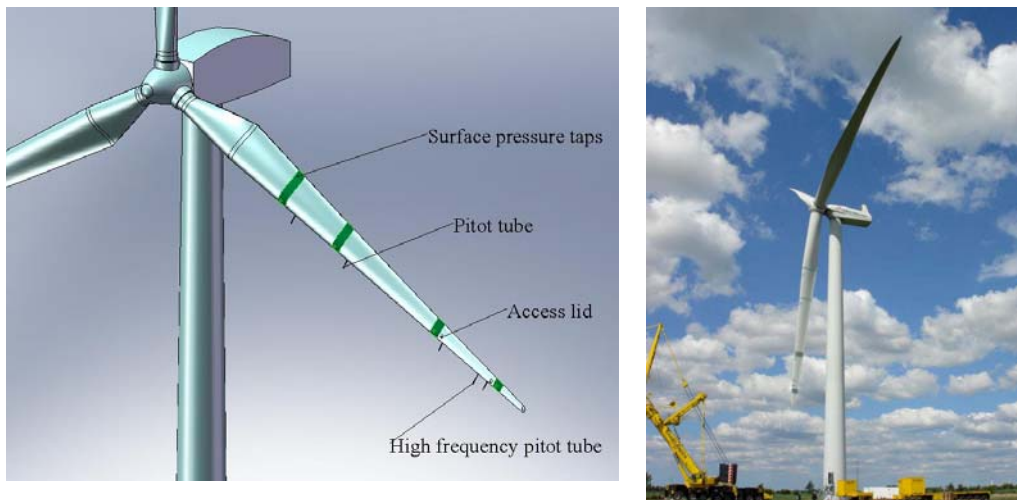
Chord length

	Pos 10e: 3.0m
	Pos 10D: 3.6m
	Pos 10C: 4.0m
	Pos 10B: 4.5m
	Pos 10A: 5.0m
	Pos 9: 6.0m
	Pos 8C: 9.0m
	Pos 8B: 9.4m
	Pos 8A: 10.0m
	Pos 7: 14.0m
	Pos 6: 18.0m
	Pos 5B: 19.7m
	Pos 5A: 21.0m
	Pos 4: 24.0m
	Pos 3B: 25.5m
	Pos 3A: 27.0m
	Pos 2: 32.0m
	Pos 1: 37.0m

R_tip - r

LM38.8

Legend:
— Leading edge
— Trailing edge
— Surface pressure taps
— Pitot tube
····· Pitot tube (high frequent)
– – Strain gages and accelerometer
— Access lid

Figure 5 Radial position of the instrumentation of the LM38.8 blade.

Figure 6 Sketch of the instrumented LM38.8 m blade to the left and to the right the NM80 turbine with the test blade installed on May 13 2009.

Figure 7 To the left: about 50 microphones were installed about one mm below the blade surface at the outboard section at radius 37 m for high frequency surface pressure measurements. The boring from the microphones to the blade surface has a diameter of 1.5 mm. To the right: every evening all pressure taps, microphones and five hole pitot tubes were covered with tape to protect against moisture and rain.

Figure 8 The local inflow at four radial positions was measured with four five hole pitot tubes sticking out from the leading edge of the blade.

Figure 9 Map of the site (maps.google.dk). The site is app. 10 km east-south-east of Esbjerg. The site has eight wind turbines of the size around 2MW. The position of the NM80 is shown together with the other 7 turbines on the site. Also the position of the meteorology mast is shown.

The test turbine is situated in a small wind farm at Tjaereborg close to the west cost of Jutland about 1 km from the North Sea, Figure 9. In total the wind farm has 8 turbines placed in two rows which gives different single and multiple wake situations with the

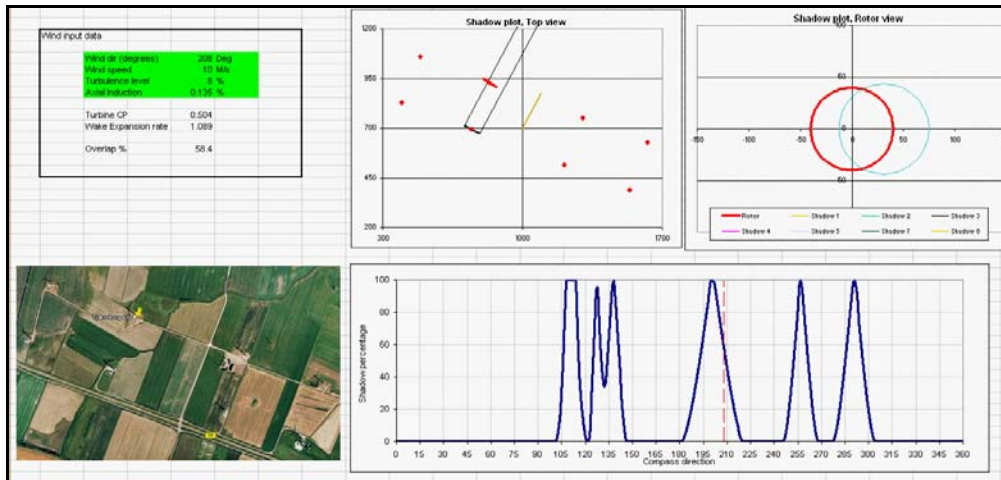closest spacing about 3.5 turbine diameters, Figure 10, provided by Vestas, N.A.Olesen Vestas [6].

Figure 10 Illustration of the wake situations occurring from different wind directions.

3 Results from wind tunnel experiments

During the project a number of wind tunnel measurements were carried on different airfoil sections, with different instrumentation and in three different wind tunnels: the VELUX wind tunnel (DK), the LM Glasfiber Low Speed Wind Tunnel (DK) and the Delft Low Speed Low Turbulence wind tunnel (NL).

Velux

- measurement of polars using pressure taps and a wake rig

- measurement of turbulence in the tunnel with hot wire equipment and a pitot tube with microphones

- measurement of high frequency surface pressure fluctuations for studying transition and aeroacoustic source terms

LM

- measurement of polars using pressure taps and a wake rig

- measurement of turbulence in the tunnel with hot wire equipment and a pitot tube with microphones

- measurement of high frequency surface pressure fluctuations for studying transition and aeroacoustic source terms

- modifying tunnel turbulence by introducing a turbulence grid

Delft

- measurement of polars using pressure taps and a wake rig

A considerable amount of data has been measured during these measurement campaigns but most of the data have not yet been analyzed in details. However, a few examples of processed data will be presented below.

3.1 Comparison of polars from different wind tunnels

One of the main objectives of the wind tunnel part of the project was to investigate the difference in polars for the same airfoil section measured in different wind tunnels. Results on this have been presented by Bak et al.[7] and a short summary of the data is presented below.

The NACA 63_3-418 airfoil originally designed for airplanes but commonly used on wind turbines and the wind turbine dedicated high lift airfoil Risø-B1-18 were the two airfoils used in the investigation. One NACA 63_3-418 airfoil model and one Risø-B1-18 airfoil model with chord length 0.60 m were used in both the VELUX tunnel and the Delft tunnel. For the LM Glasfiber tunnel new models were manufactured with a chord length of 0.90 m. Tests were carried out at Re=1.5x10^6 and 1.6x10^6. For the Delft and LM tunnel Re=3x10^6 was also tested. Different configurations were tested such as clean surface and leading edge roughness in terms of zigzag tape at the leading edge.

The polars for the NACA 63$_3$-418 airfoil at $Re=1.5x10^6/1.6x10^6$ in clean configuration and with leading edge roughness are shown in Figure 11 and Figure 12, respectively. The best correlation between the data from the different tunnels is seen for the case with leading edge roughness.
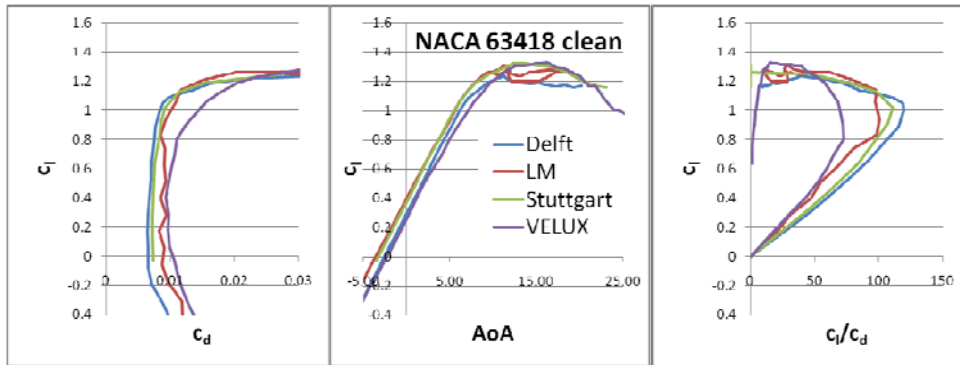

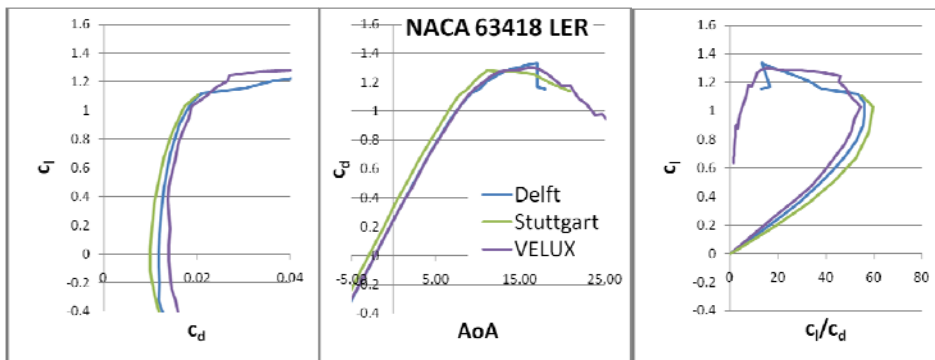*Figure 11 Polars for NACA63$_3$-418 airfoil at $Re=1.5x10^6$ to $1.6x10^6$ in clean configuration.*

Figure 12 Polars for NACA63$_3$-418 airfoil at $Re=1.5x10^6$ to $1.6x10^6$ with leading edge roughness (LER).

The comparison of the data from the different tunnels for the Risø-B1-18 airfoil shown in Figure 13 and Figure 14 at Re=1.5x106/1.6x106 reveals bigger deviations for the maximum lift as seen for the NACA633-418 profile. The Risø-B1-18 airfoil has a higher maximum lift coefficient than the NACA633-418 airfoil and this probably makes it more sensitive to the specific test conditions in the different wind tunnels.
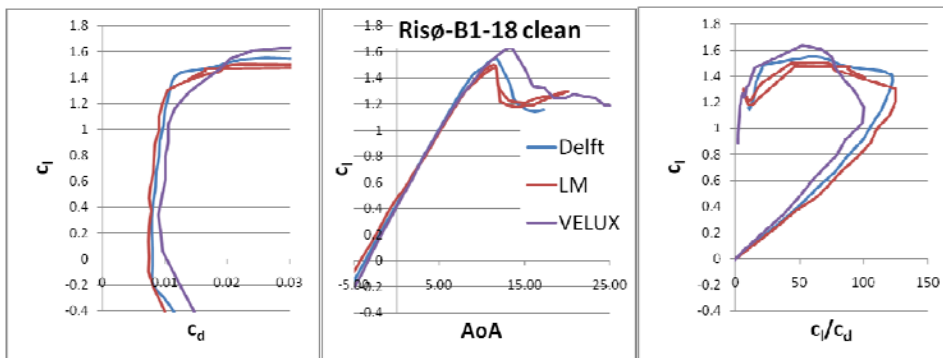

Figure 13 Polars for Risø-B1-18 airfoil at $Re=1.5x10^6$ to $1.6x10^6$ in clean configuration.

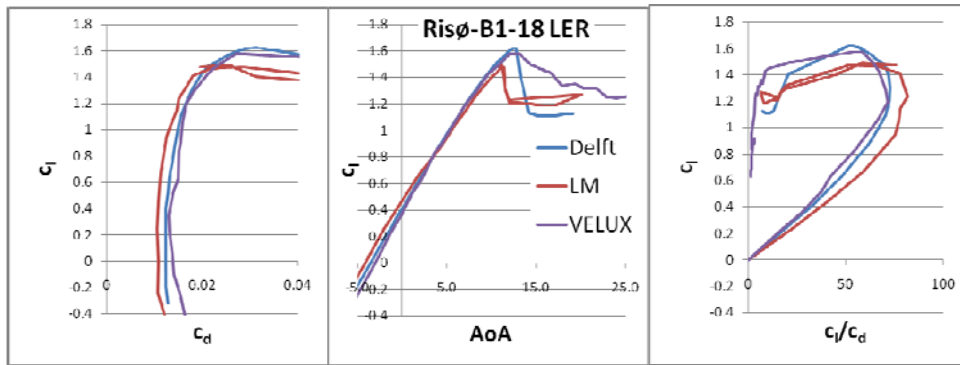*Figure 14 Polars for Risø-B1-18 airfoil at Re=1.5x10^6 to 1.6x10^6 with leading edge roughness.*

For both the NACA 63$_3$-418 and the Risø-B1-18 airfoil it should be noted that the applied leading edge roughness (LER) (zigzag tape mounted on suction side at x/c=0.05 from the leading edge and on pressure side at x/c=0.10 from the leading edge) in the test case presented in Figure 12 and Figure 13 does not decrease the maximum lift coefficient $C_{l\max}$ but even increases $C_{l\max}$ slightly, in particular for the measurements in the Delft tunnel. Other more severe leading edge roughness configurations were tested in the project where the expected decrease in $C_{l\max}$ was observed. The mechanism behind the slightly increase in $C_{l\max}$ in the present case could be that the zigzag tape, which simulates the roughness, works as small vortex generators thereby strengthening the boundary layer with an increase in c_{lmax} as result.

3.2 Polars for sections of the LM38.8 blade

Another important objective with the wind tunnel measurements was to test airfoil sections with the same geometry as the four instrumented sections on the full-scale LM38.8 blade on the NM80 turbine in Tjæreborg. The section geometry on the LM38.8 blade was measured with a laser instrument and afterwards four wind tunnel airfoil sections were manufactured and tested in the LM wind tunnel. Again the tests were performed for different Reynolds numbers and for different configurations of leading edge roughness. As an example, results for the three inner sections, sec. 03 at radius 13.0 m (32.5% of rotor radius), sec. 05 at radius 19.0 m (47.5% of rotor radius) and sec. 08 at radius 30.0 m (75.0% of rotor radius) are shown in Figure 15. The airfoil thicknesses for the three sections are 33.3% for sec. 03, 24.0% for sec. 05 and 18.9% for sec. 08, respectively.

The polars for the three different airfoils differ in particular for their different dependency on the roughness. The C_l curve for the 33% airfoil for the two most severe roughness conditions has a slope much lower than for the clean airfoil and indicates separated flow. Also the maximum lift coefficient for 24% thick airfoil is considerable lower when roughness is applied while the 18.9% thick airfoil has only a low dependency on the roughness.
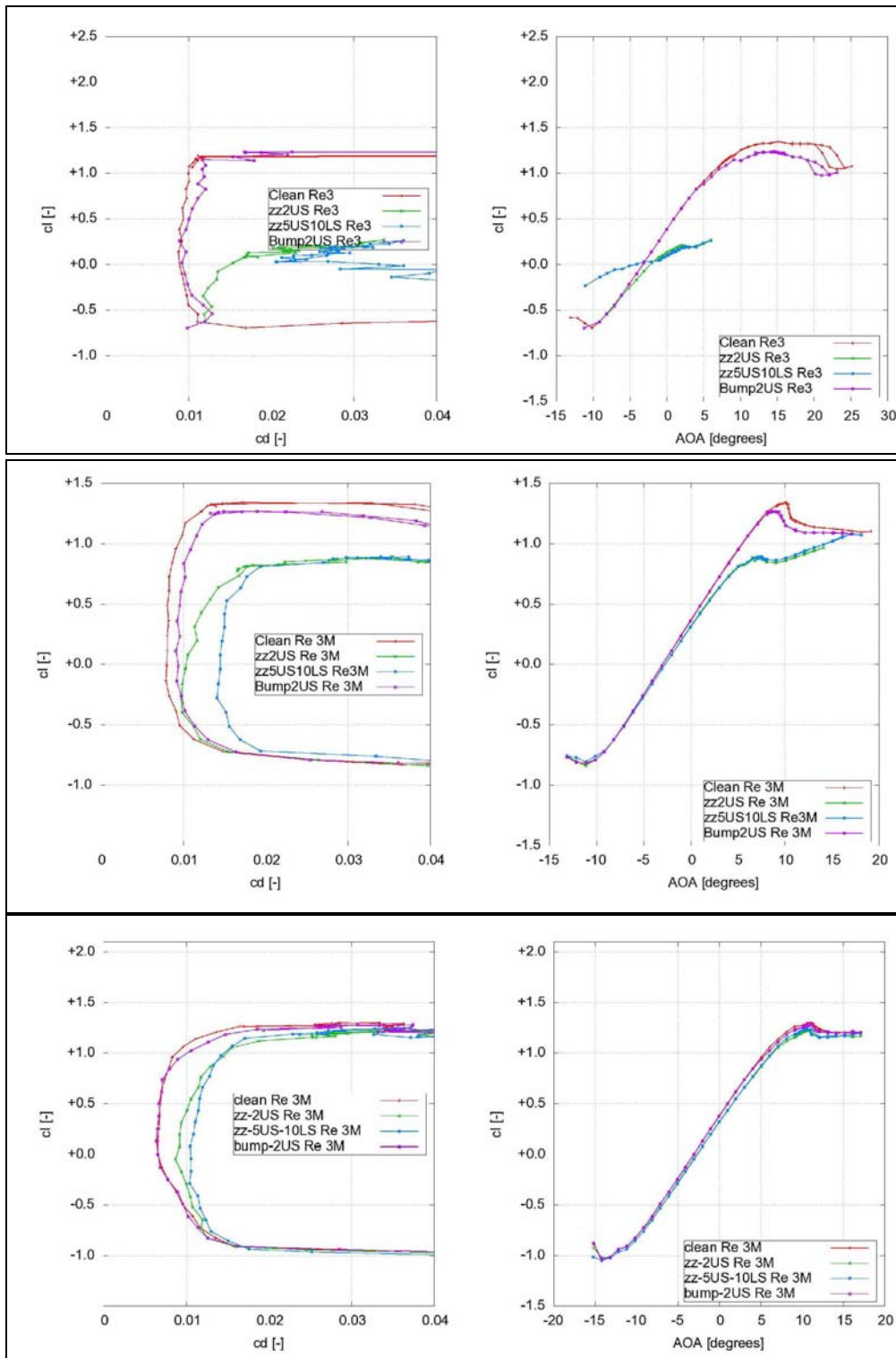
Figure 15 Polars for the three inner sections of the LM38.8 blade measured in the LM wind tunnel. Top figure: sec.03 at 33% of rotor radius; mid figure: sec.05 at 48 % of rotor radius and bottom figure: sec. 08 at 75% of rotor radius.

3.3 Surface pressure fluctuations measured with microphones

The measurements of high frequency surface pressure fluctuations with microphones have two main objectives:

- detection of position of transition
- determining acoustic noise sources

The power spectra of the surface pressure fluctuations are quite different for a laminar and a turbulent boundary layer. In particular in the frequency range from e.g. 1 kHz to 10 kHz the difference is considerable and this is illustrated in Figure 16 where the PSD spectrum for the microphone at position 13.8% from the leading edge is much higher than the spectrum for the microphone at position 10.2%. So, the transition has been detected to be within these two positions.
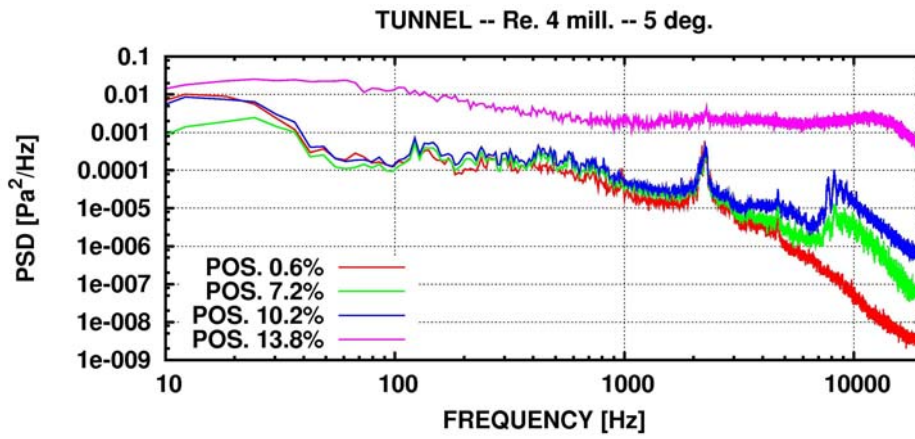

Figure 16 Test of the outboard section of the LM38.8 blade in the LM wind tunnel. The figure shows the power spectrum of the signal from four microphones in the leading edge region of the airfoil, and the transition is detected to be between position 10.2% from the leading edge and position 13.8%.

The surface pressure fluctuations close to the trailing edge are the source of the trailing edge noise and thus also an important intermediate result in a noise prediction model for prediction of the far field noise. Measurements of the power spectrum of the pressure fluctuations can thus be used to validate and tune noise prediction models. An example of this type of measurement is shown in Figure 17, where the spectrum for a microphone at about 85% from the leading edge is shown for different angle of attacks. The general tendency in the spectrum for an increasing angle of attack is that the energy increases at the lower frequencies and decreases in the other end of the spectrum due to the increasing thickness of the boundary layer. The considerable peak at around 5 kHz is a distinct noise from the wind tunnel.
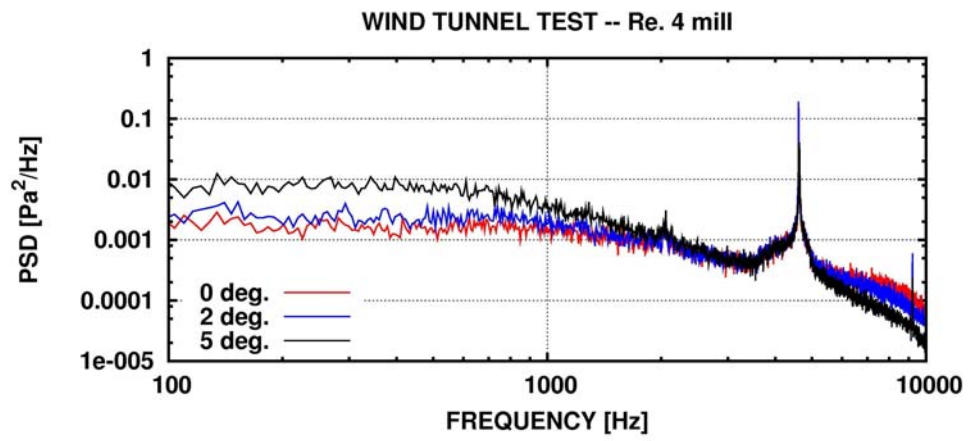
Figure 17 Power spectrum for the microphone around 85% position from the leading edge at three different angle of attack.

4 Inflow measurements on the Siemens 3.6 MW turbine at Høvsøre

4.1 General description

The pitot tube was mounted in the beginning of March 2007, but at that time the Risø data acquisition system was not connected to the data channels from the turbine. Later it was decided to connect a few of the turbine parameters (e.g. rpm., pitch, electrical power) to the Risoe data acquisition system. This has been in operation from spring 2009 to the end of the project period.

During the whole measurement period, the pitot system has been purge manually several times. Calibration of the pressure transducers has also been carried out.

To summarize there are the following two main measuring periods:

1. From March 2007 to the end of 2008 only the pitot tube channels were sampled with the Risoe data acquisition system. The turbine data and meteorological data were sampled with the Siemens system and it is possible to synchronize the two set of data files. However, it seems to be difficult to carry out an exact synchronization of the signals during time and even within the time frame of one day.

2. Data from week 20 to week 43 2009, where the pitot channels and the turbine channels are in the same files. A statistical analysis (10 min. statistics) of these data has been performed and summarized in graphs covering one week. See an example below in Figure 18 for hub wind speed and inflow angle. It should be noted that the off-set of the measured local inflow angle has not been calibrated in this first analysis.
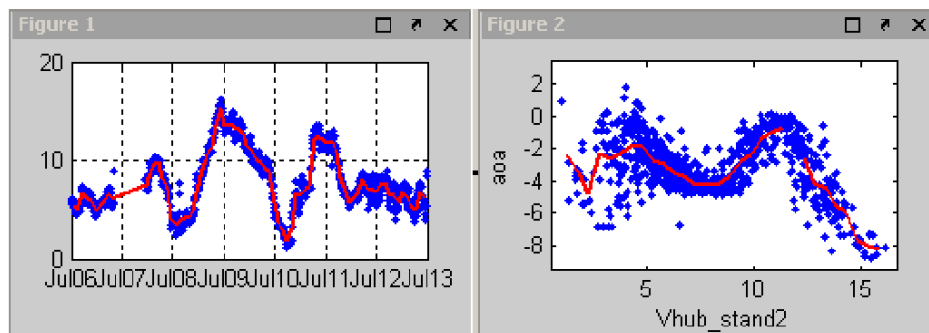

Figure 18 10 min. average values of wind speed at hub height from the meteorology mast west of the Siemens 3.6 MW turbine and the local inflow angle (off-set not calibrated) measured with the pitot tube on the blade of the Siemens turbine, shown as function of hub wind speed.

4.2 Example of inflow measurements

The following figures are intended to show the quality of the inflow measurements with the five hole pitot tube. The presented data set was arbitrarily selected from May 18 2009, where the wind speed and wind direction from one of the met masts at Høvsøre are shown in Figure 19.
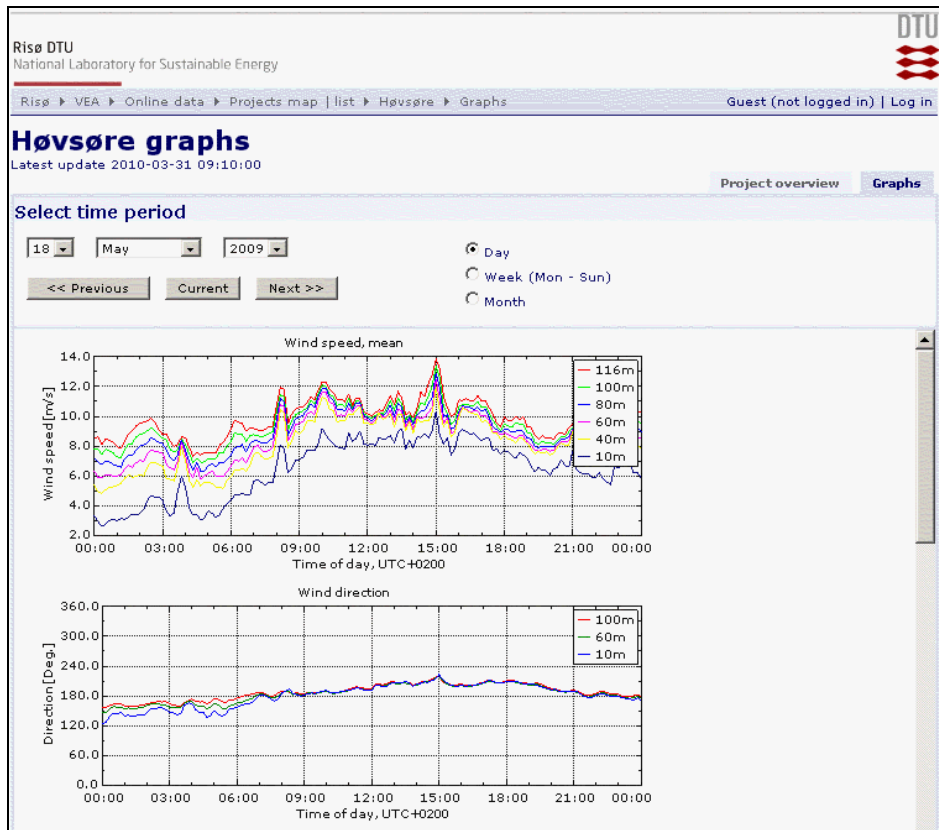
Figure 19 Wind speed and wind direction at Høvsøre on May 18 2009, where the inflow data presented Figure 20 are from 11 o'clock this day. Graph is from http://veaonline.risoe.dk/.

The measured inflow angle and relative velocity for a 10 min. period is shown in Figure 20. In order to illustrate the major 1p content in the signals due to wind shear and the instantaneous yaw error, the low pass filtered signals with a cut-of frequency of 0.2 Hz are shown in Figure 21. Finally the good correlation between the measured relative velocity, low pass filtered in this case with a cut of frequency of 0.1 Hz, is compared with the generator speed in Figure 22.
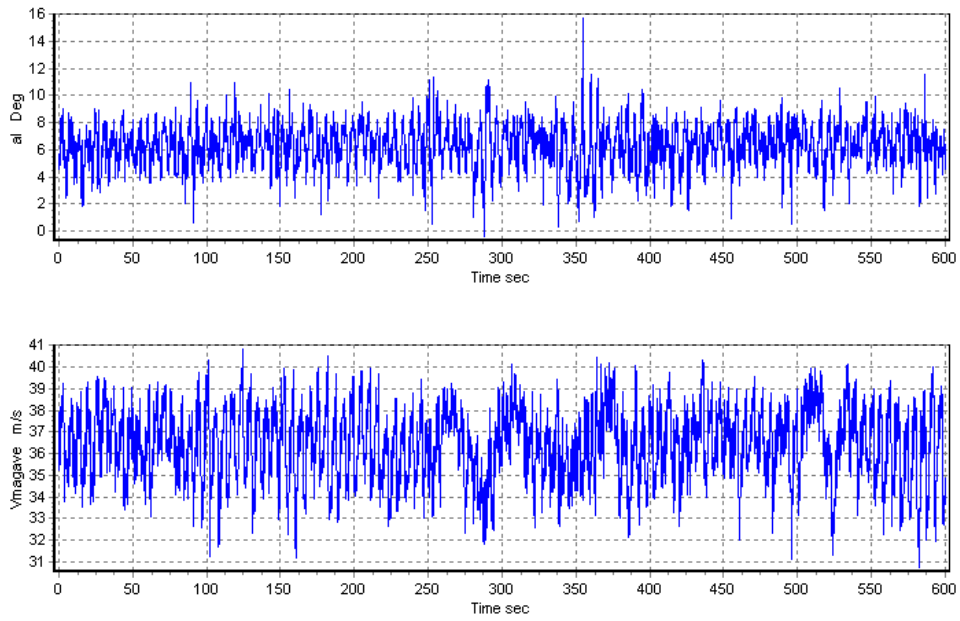
Figure 20 Local inflow angle (top) and relative velocity (bottom) measured with the five hole pitot tube on May 18 2009 at 11 o´clock.
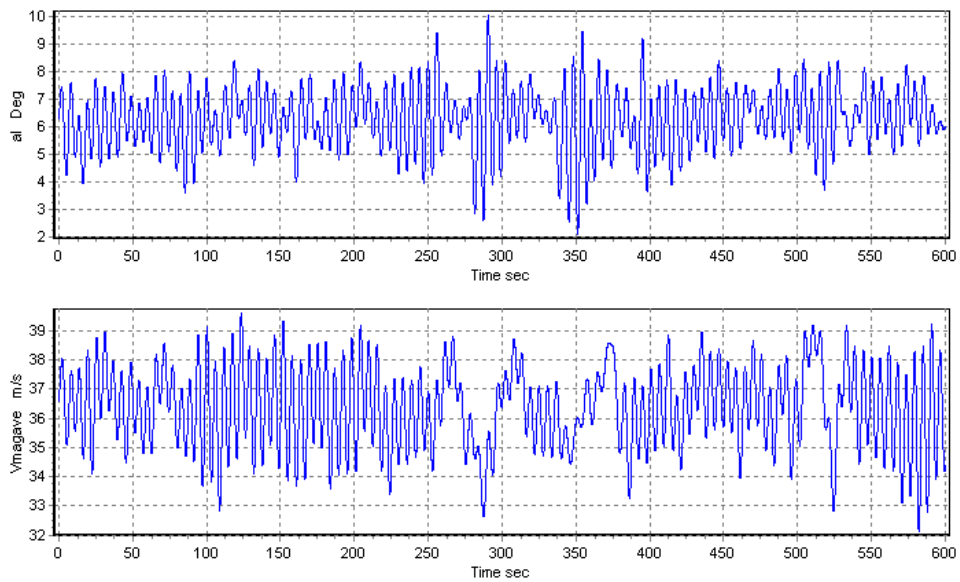

Figure 21 The same data as shown in Figure 20 but now low pass filtered with a cut off frequency of 0.2 Hz in order to show the 1p variations in the signals.
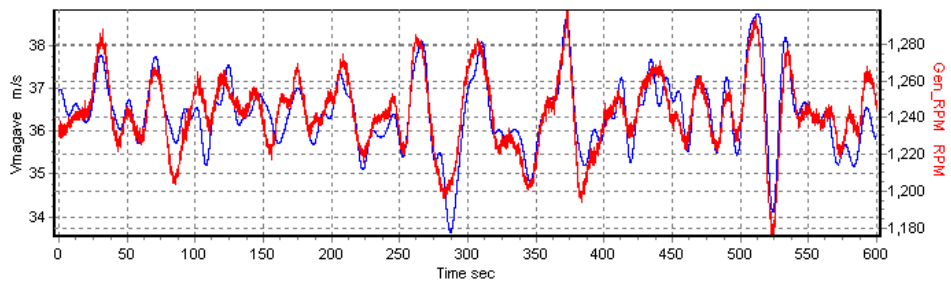

Figure 22 The relative velocity low pass filtered with a cut-off frequency of 0.1 Hz and shown in comparison with the generator speed.

4.3 Derivation of wind shear and turbulence from inflow data

One major application of inflow data is the derivation of wind shear and turbulence characteristics from the data. A method for this has been presented by Madsen and Fischer [8] and a few results from this work will be presented here.

The data presented are all from one day on March 28 2007. In a longer time period around this day the weather was clear and sunny with temperatures around 15 °C during daytime and close to 0°C in the night. These weather conditions caused a very stable boundary layer to develop during the night with a strong shear and low turbulence. An example of measured inflow angle at night and at daytime, respectively, is shown in Figure 23. During night a considerable 1p variation is seen in the inflow signal, whereas the pattern is much more stochastic during daytime.
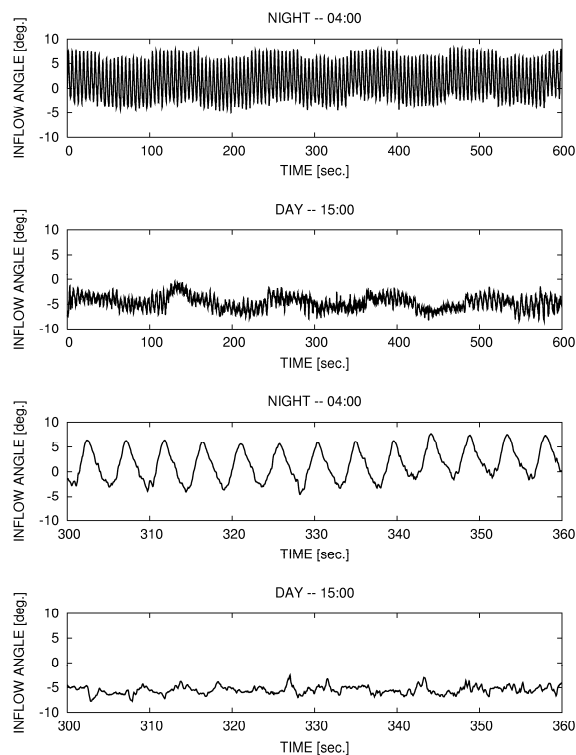
Figure 23 A comparison of inflow angle measured at night and at day, respectively, showing the influence of strong wind shear and low turbulence during night.

The method for derivation of the wind shear profile from inflow data is based on an aerodynamic simulation (in this case the HAWC2 code), where shear is superposed on the inflow to the simulation and adjusted to give the same azimuthal variation in local inflow angle as measured, Figure 25. The shear applied in the simulation is then the shear derived from the inflow measurements and can be compared with the shear measured in a met mast. As seen in Figure 24 the correlation is quite good.
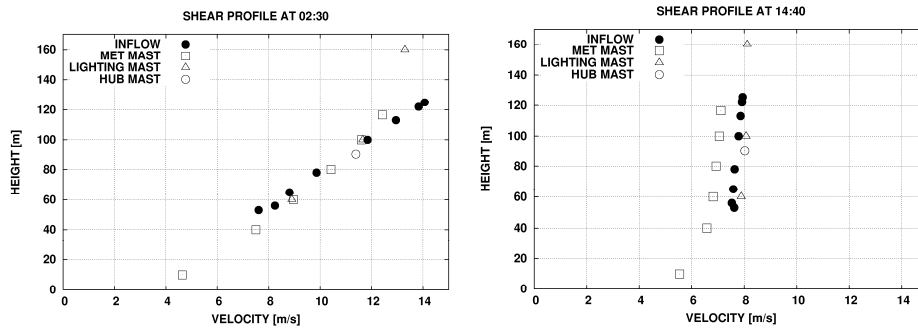
Figure 24 Wind shear profile derived from inflow data and compared with profiles from different masts nearby.
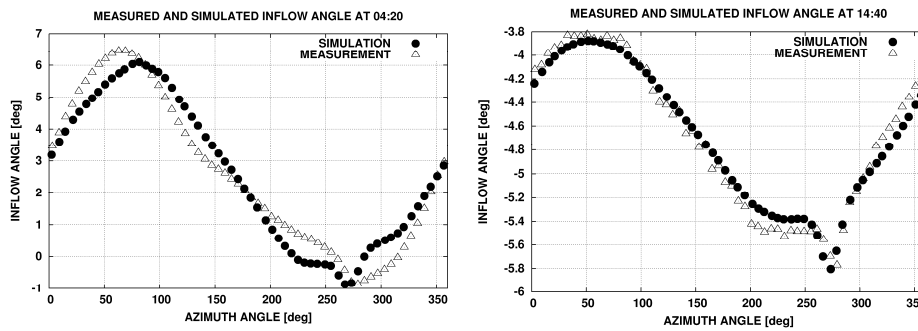

Figure 25 The inflow pofiles (inflow angle as function of azimuth position) used for derivation of the wind shear profiles in Figure 24.

Likewise the turbulence can be derived from inflow data by correlating the standard deviation of the computed local inflow angle with the measured ones and in this case adjusting the local turbulence intensity in the inflow to the simulation, Figure 27. The applied local turbulence intensity in the simulations can then be compared with the turbulence measured in the nearby meteorology masts, Figure 26. For the night case the correlation is good, whereas the deviations are bigger for the case during daytime. However, there is also a big deviation between the turbulence data measured in two masts at that time as can be seen in Figure 26.
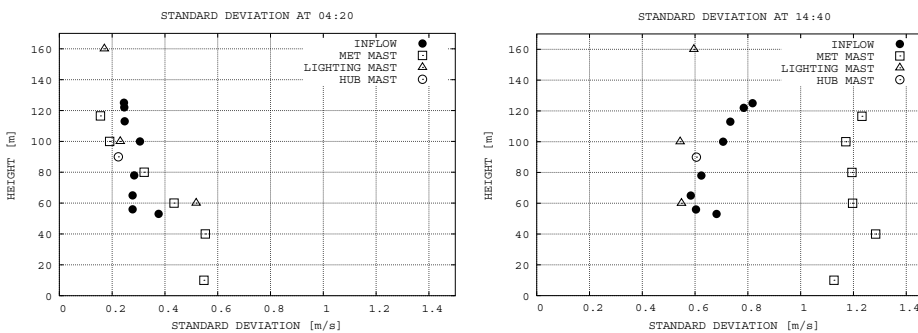

Figure 26 Turbulence profiles derived from inflow data and compared with profiles from different masts nearby.
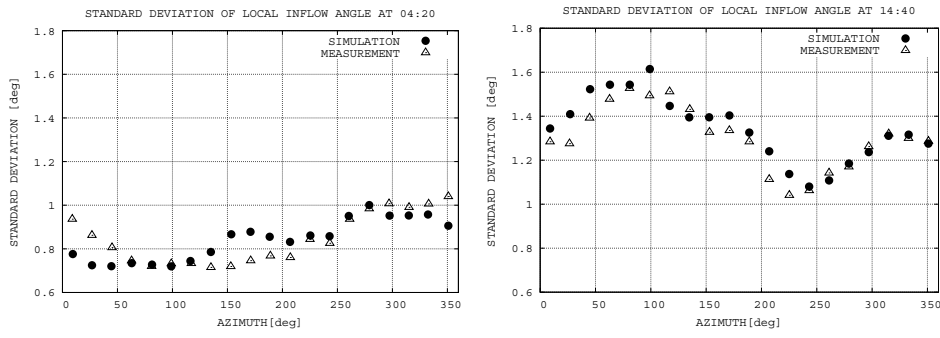
Figure 27 The inflow pofiles of standard deviation as function of azimuth position used for the turbulence profiles in Figure 26.

5 Pressure and inflow measurements on the NM80 turbine in the Tjæreborg wind farm

5.1 Types of data

Measurement campaigns were conducted from late June 2009 to mid September 2009. Sensors on the turbine and in the meteorology mast were sampled with one separate data acquisition system with 35 Hz for 10 min., while the pressure taps were sampled with 100 Hz for 9 min and 30 sec and started at the same time as the 35Hz measurements. The microphones were sampled with 50 kHz over a 10 sec. period and with a new sampling started each minute. Besides the pressure, inflow and microphone sensors a considerable number of strain gauges and accelerometers mounted on the blades, the shaft and the tower were sampled, also with a frequency of 35 Hz. Finally a number of meteorological sensors mounted in a 90 m mast close to the turbine were also sampled with a frequency of 35 Hz.

The data were thus sampled with three different systems and three different scan rates. However, one trigger signal was sampled in all three systems so an exact merging of the files can be performed afterwards. An example of this is shown below in Figure 28, where a microphone signal sampled with 50 kHz is merged together with a signal from the five hole pitot tube sampled with 35 Hz. It is seen that the microphone positioned at x/c=0.056 from the leading edge of the blade shows reduced response (laminar flow) when reducing the inflow angle and increased response (turbulent flow) when increasing the inflow angle.
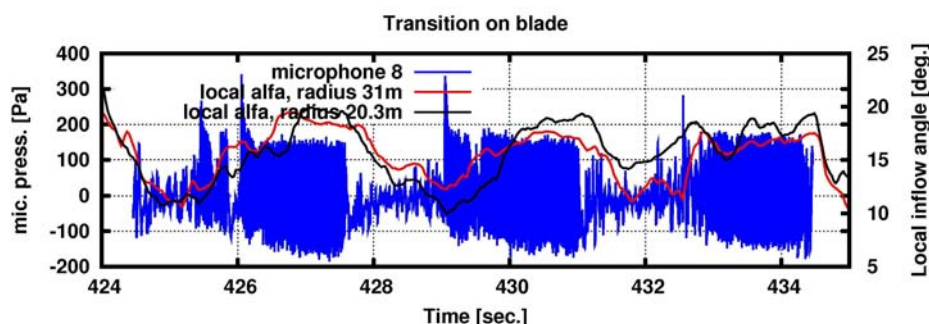

Figure 28 An example of merging different file types. In this case a microphone signal (blue curve) scanned with 50 kHz and the inflow angle (red curve) scanned with 35 Hz.

5.2 Example of data for studying 2D/3D airfoil characteristics

An initial comparison of 2D pressure distributions (from the LM wind tunnel) and 3D pressure distributions (measured on the NM80 rotor) for the root and tip section of the LM38.8 m blade at 13% radius and 93% radius, respectively, has been presented by Madsen *et al.* [9] and Bak *et al.* [10] and a few results from this work will be shown here. The pressure distributions from the rotor were averaged over a period of 30 sec. with the turbine operating at 10-12 m/s. The raw voltage data from the pitot tubes has not yet been converted to inflow angle, which therefore was estimated from BEM simulations. The dynamic pressure used for non-dimensionalization was derived from the velocity triangle with the rotational blade section velocity and a local axial velocity assuming an induction factor of 1/3. However, for the inboard section an additional factor of 1.25 was applied on the dynamic pressure in order to obtain a reasonable

correlation of the rotor pressure distribution with the 2D data and the 3D CFD pressure distributions. One cause of this deviation could be the contribution to the relative velocity from the swirl which was not included. However, in the future analysis the dynamic pressure will be derived from the inflow velocities from the adjacent five hole pitot tubes. Finally, the mean level of the pressure distributions were chosen to fit the pressure peak on the pressure side of the airfoil to the 2D pressure distributions.

Comparing now the pressure distributions in Figure 29 it is seen that for sec. 4 at 93% radius there is a close correlation with the 2D wind tunnel data and with the 3D CFD data at 11 m/s. It should be noted that the CFD blade geometry data are based on the exact NACA 634xx geometry whereas the wind tunnel section model is a copy of the measured geometry of the rotor section. In the leading edge region and up to around 25% position there is an indication in both the rotor and 2D pressure distribution of a slightly modified airfoil geometry.

For the inboard section at 33% radius a systematic deviation between the 3D pressure distributions from the rotor and the 2D pressure distributions are seen. In particular the deviations are found on the front part of the airfoil section with attached flow. However, the 3D CFD pressure distributions are generally closer to the pressure distributions measured on the rotor than in the wind tunnel. Further the CFD simulations show considerable flow separation on the inboard part of the blade as seen in the streamline plot in Figure 30.
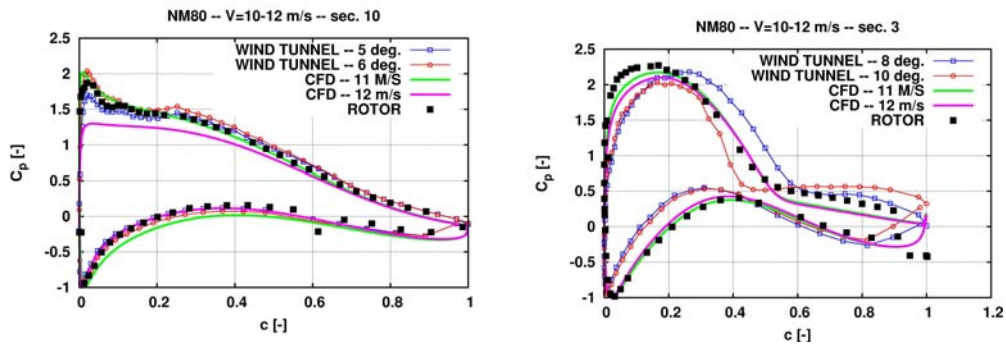

Figure 29 Measured pressure distributions, on the rotor and in the LM wind tunnel, on two sections of the LM38.8 blade, the most outboard section of the blade named sec. 4 and the most inboard section named sec. 1, in comparison with pressure distributions computed with the CFD code EllipSys3D.
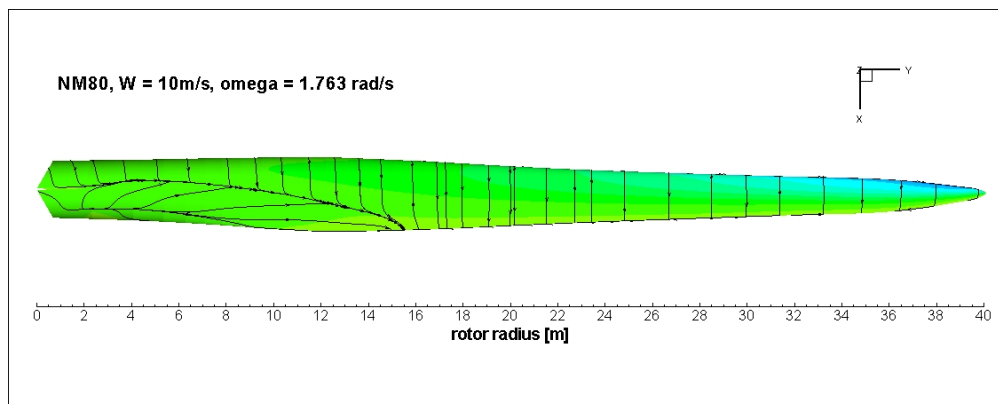

Figure 30 Computed streamlines with the ElliSys3D code at a wind speed of 10 m/s showing separation at the inboard section at radius 13 m.

5.3 Example of comparing transition on the rotor with transition in the LM wind tunnel and influence of turbulence in inflow

From the same study as referenced above, Madsen et al. [9] and Bak et al. [9a], spectra of surface pressure fluctuations measured on the rotor, measured on the section in the wind tunnel and measured in the wind tunnel with a turbulence grid are compared for different microphone positions, Figure 31. The turbulence grid mounted in the inlet of the LM tunnel created a turbulence level of between 1 to 2% in the test section. The measured spectra close to the leading edge are a good indicator of the turbulence in the inflow as the boundary layer on the airfoil only has developed over a short distance. Comparing the spectra at 0.6% from the leading edge it is seen that up to about 500 Hz the spectrum measured on the rotor indicates much higher inflow turbulence in this frequency range. It is also seen that the turbulence grid raises the turbulence in a frequency interval, where the rotor spectrum correlates better with the spectrum measured in the clean tunnel. However, it is seen that for the 4.7% position there is a good correlation between the rotor spectrum and the spectrum measured in the wind tunnel with the grid. For the cases at 2.3% and 4.7% chordwise positions the boundary layer is turbulent at the rotor, whereas it is still laminar in the tunnel without grid. Proceeding further downstream to position 13.8% all three boundary layers are now turbulent, but the energy in the rotor spectrum is considerable lower except at frequencies below 50 Hz.

The spectra measured close to the leading edge at the rotor indicate thus a much higher turbulence or unsteadiness in the inflow than seen in the wind tunnel flow for frequencies up to about 500 Hz. This appears also clearly when time traces of the surface pressure fluctuations are compared as shown in Figure 32. The scales in the figures are identical and the inflow velocity on the rotor and in the wind tunnel is almost the same. It is clear from the comparison in Figure 32 that the scales of the turbulence caused by the grid are too small. In future analysis of the pressure fluctuation data a key question will be to investigate what influence the much higher energy content in the inflow below 500 Hz has on transition when compared with wind tunnel conditions.
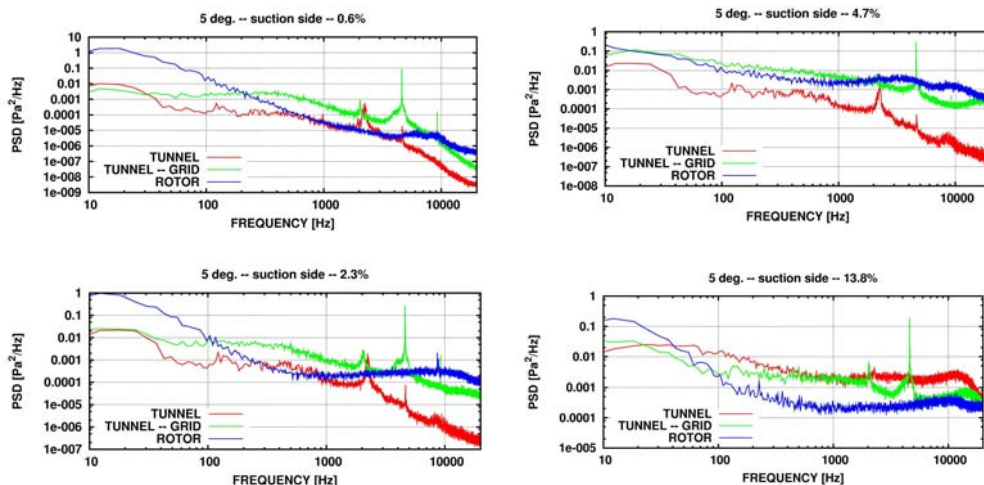

Figure 31 A comparison of spectra of surface pressure fluctuations for four positions, 0.6% (top left), 2.3% (bottom left), 4.7% (top right) and 13.8% (bottom right) from the leading edge for the airfoil section corresponding to the outermost section at the rotor in the wind tunnel without and with turbulence grid and on the rotor.
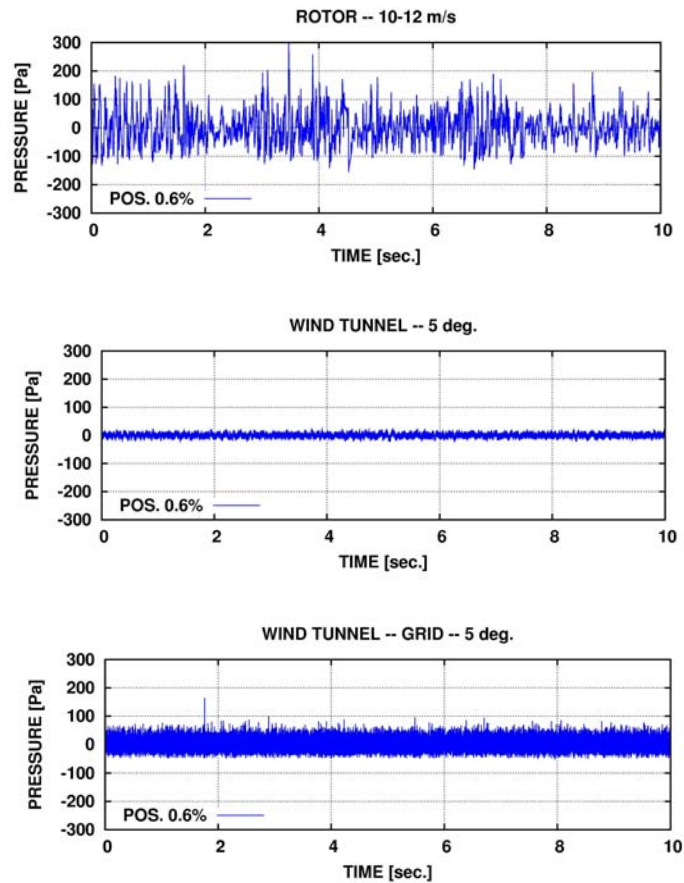
Figure 32 Time trace of surface pressure signal at 0.6% position from the leading edge measured on the rotor (top), in the wind tunnel without turbulence grid (mid) and in the wind tunnel with turbulence grid (bottom).

5.4 Example of data from wake operation

One of the objectives with the experiments was to get improved insight into the wake flow characteristics as most turbines operate close to other turbines and thus experiences inflow which is the wake flow from another turbine. As there are seven other turbines on the site, the NM80 turbine with the test blade will operate in wakes from many wind directions as shown in Figure 10. Below a number of figures will illustrate the influence of wake situations with the wind direction in an interval around 200°, where the upstream turbine is around 3.5 rotor diameters away.

During the measurement day of September 1 2009, the wind direction increased slowly from around 180° at 12 o'clock to about 220° at 16 o'clock, Figure 33. The wind speed was in the range of 10-13 m/s. First is shown inflow data from the pitot tube at 31 m radius and the flapwise moment at 19 m radius (*r/R*=47.5%) for the half wake situation at 14:30, Figure 34. Severe 1p variations are seen in both signals as the blade passes in and out of the wake. At 14:00, where the turbine is almost in a full wake it can be seen that the 1p variations are less severe, and only in short periods there are big 1p variations when parts of the blades passes somewhat outside the wake, Figure 35. In fact the blade fatigue (material constant $m = 12$) for the flapwise load is about 50% less in the full wake situation than in the half wake.
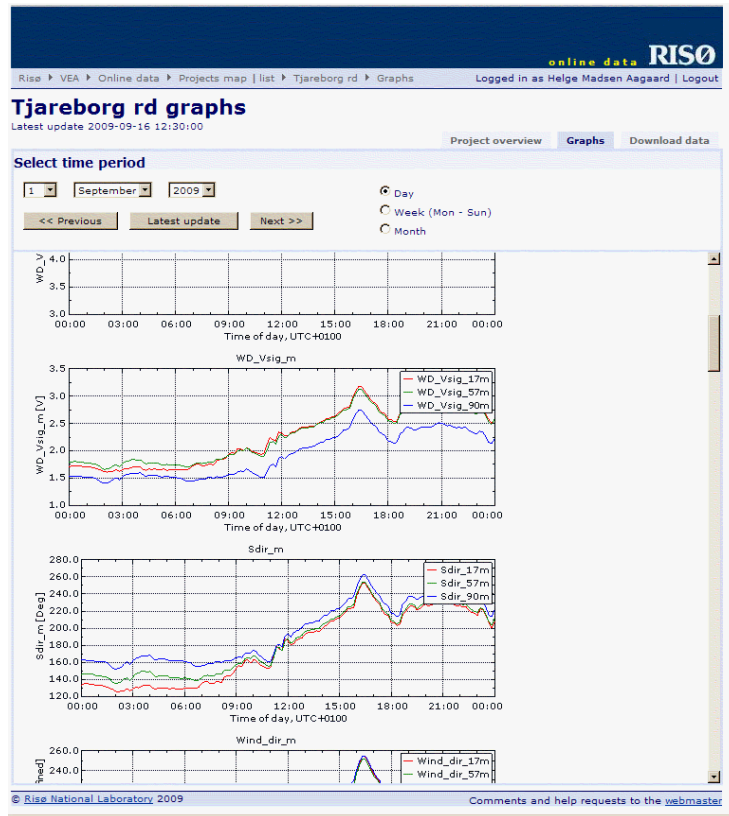
Figure 33 Wind direction on September 1 2009, resulting in a full wake situation for a wind direction of about 200 deg. at 14:00 and a half wake situation half an hour later, 14:30.
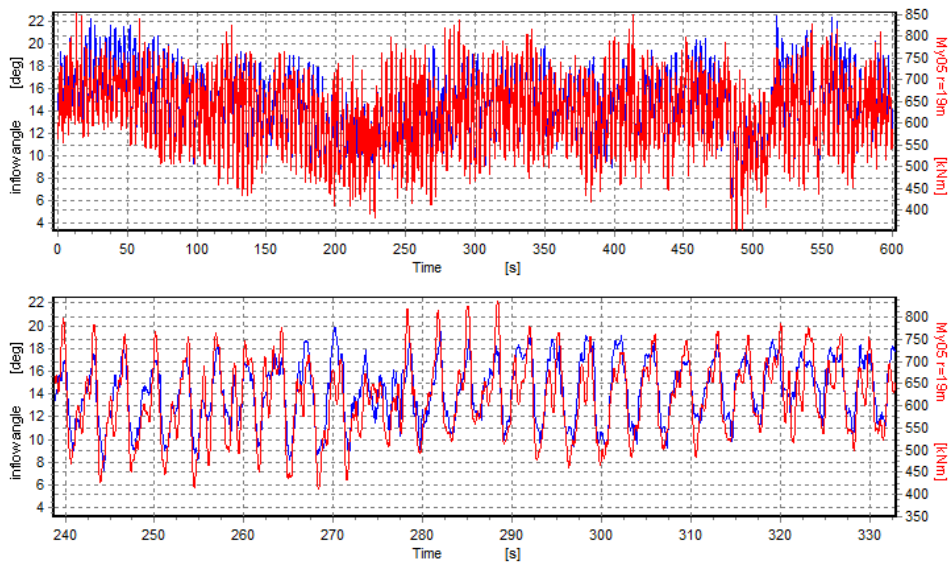

Figure 34 Data from 14:30 when the NM80 turbine operates in half wake. The blue curve is the inflow angle signal for the pitot tube at a radius of about 31 m and the red curve is the blade moment flapwise signal at a radius of 19 m.
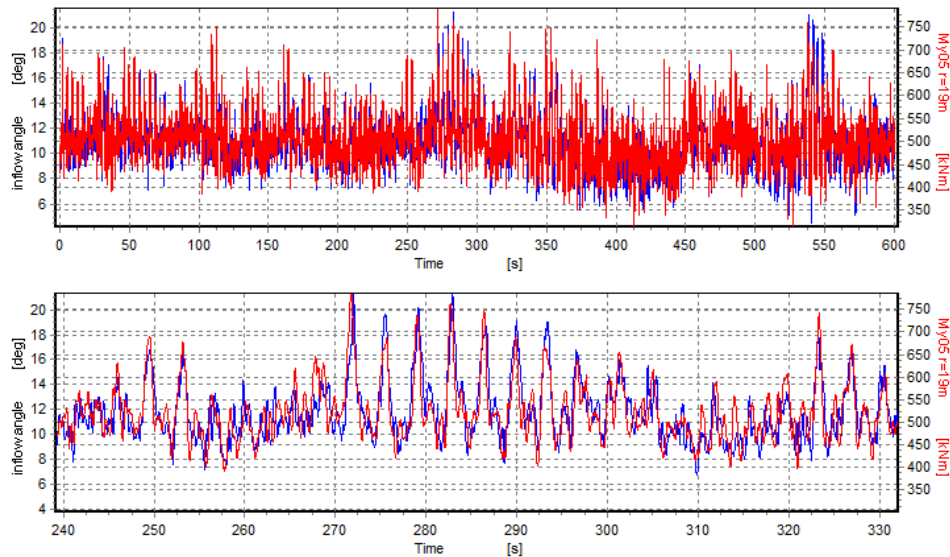
Figure 35 Data from 14:00 when the NM80 turbine operates in almost full wake. The blue curve is the inflow angle signal for the pitot tube at a radius of about 31 m and the red curve is the blade moment flapwise signal at a radius of 19 m.

5.5 Example of measurements in yawed flow

Operation in yaw causes a complex flow and induction around the rotor. Several yaw test cases were therefore contained in the test plan and it is expected that with the detailed instrumentation of the rotor new insight in yaw aerodynamics will be obtained from the present data set.

In Figure 36 the wind direction and yaw position is shown and a yaw error of about 40° can be derived from this figure. The electrical power and the inflow angle signal from the pitot tube at radius 20.3 m is shown and a severe 1p variation is present in this signal due to the yaw error. The flapwise moment at the root and at a section close to the tip is shown as a function of azimuth angle in Figure 38. Finally the blade root moment is shown for two yaw errors in Figure 39.
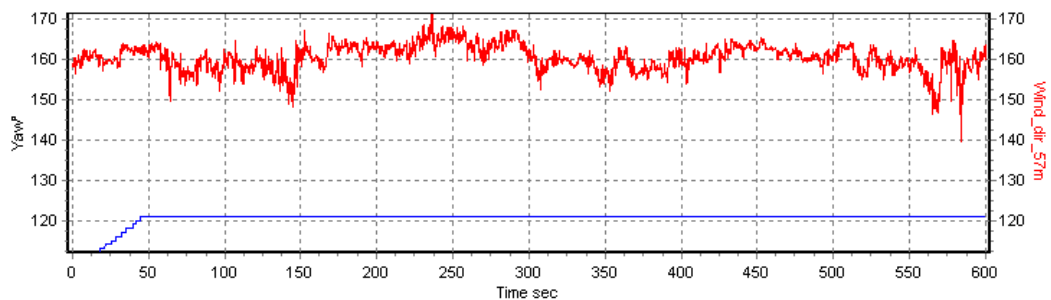

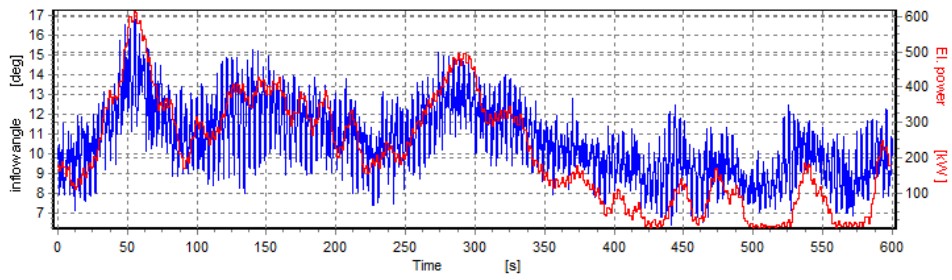*Figure 36 Yaw position (blue curve) and wind direction (red curve).*

Figure 37 The Blue curve is inflow signal from pitot tube at radius 20.3 m and the red curve is the turbine electrical power.
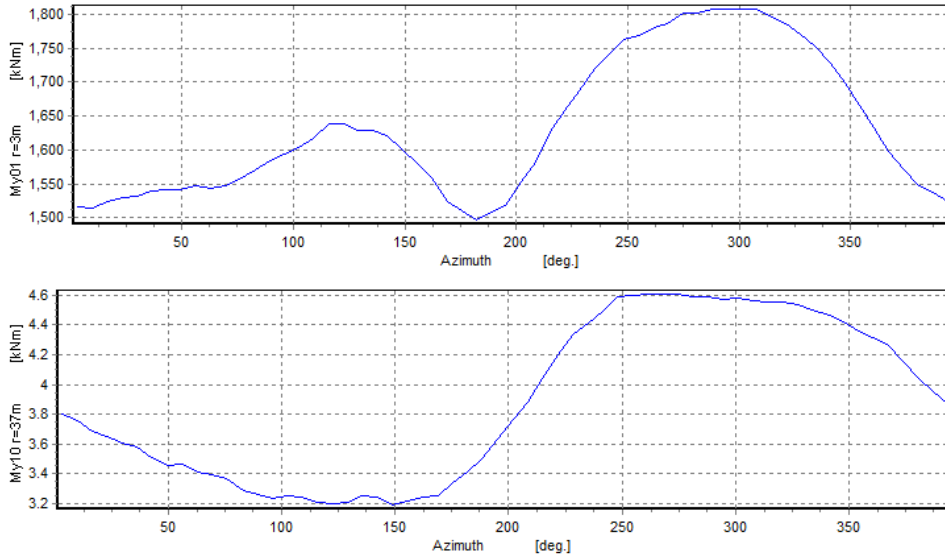

Figure 38 Top plot shows the variation of the flapwise blade root moment (radius 3 m, r/R=7.5%) as function of azimuth position and the bottom plot is for the flapwise blade moment in a cross section close to the tip (radius 37.0m, r/R=92.5%). 0° is for the blade pointing vertical upwards.
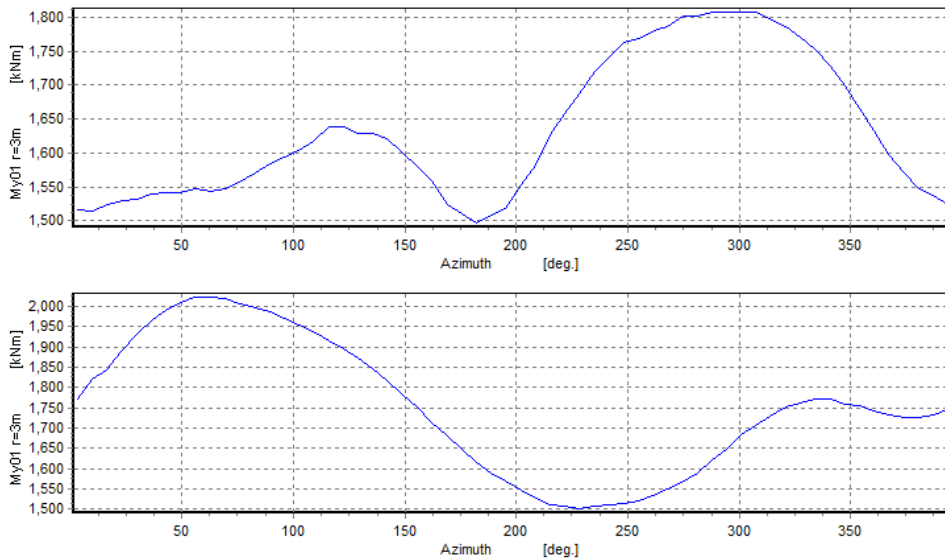

Figure 39 Comparison of the flapwise blade root moment (radius 3 m) for two cases with a yaw error of around 50 deg and -70 deg.

5.6 Example of pitch step

During a few runs the turbine was configured to make step changes in pitch with +/-1°. These measurements were carried out to provide important information for tuning the dynamic induction constants in the engineering BEM type models.

An example is presented below from measurements on September 9 at 16:20. In Figure 40 is shown the local inflow angle signal from the pitot tube at radius 31 m and the flapwise response at a cross section close to the tip (r=37.0m, r/R=92.5%) is shown next in Figure 41. Finally, a low pass filtered inflow angle is compared with the rotor power in Figure 42.
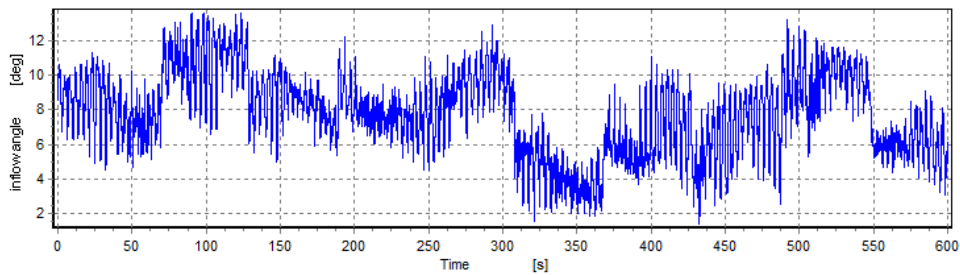

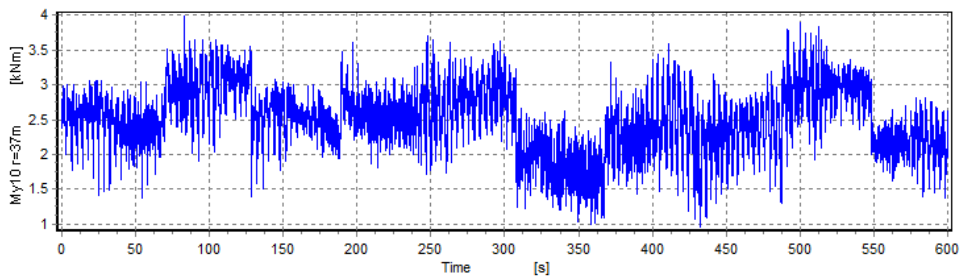*Figure 40 Local inflow angle from pitot tube at 31 m radius.*

Figure 41 Flapwise moment at a cross section close to the tip, r=37.0 m.
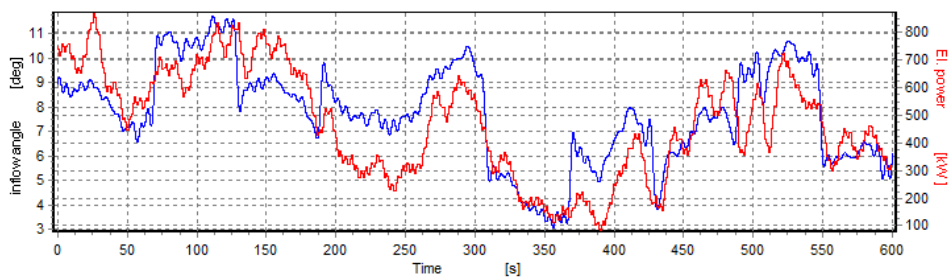

Figure 42 The local inflow angle as shown in Figure 40 (blue curve), but low pass filtered with a cut-off frequency of 0.2 Hz in comparison with the electrical power (red curve).

5.7 Example of trailing edge noise source measurements

As mentioned before the measurements of high frequency surface pressure fluctuations with the microphones are used; 1) to detect position of transition and 2) to study aeroacoustic noise sources, mainly turbulent inflow noise and turbulent boundary layer trailing edge noise. An example of the last application is shown below in Figure 43.
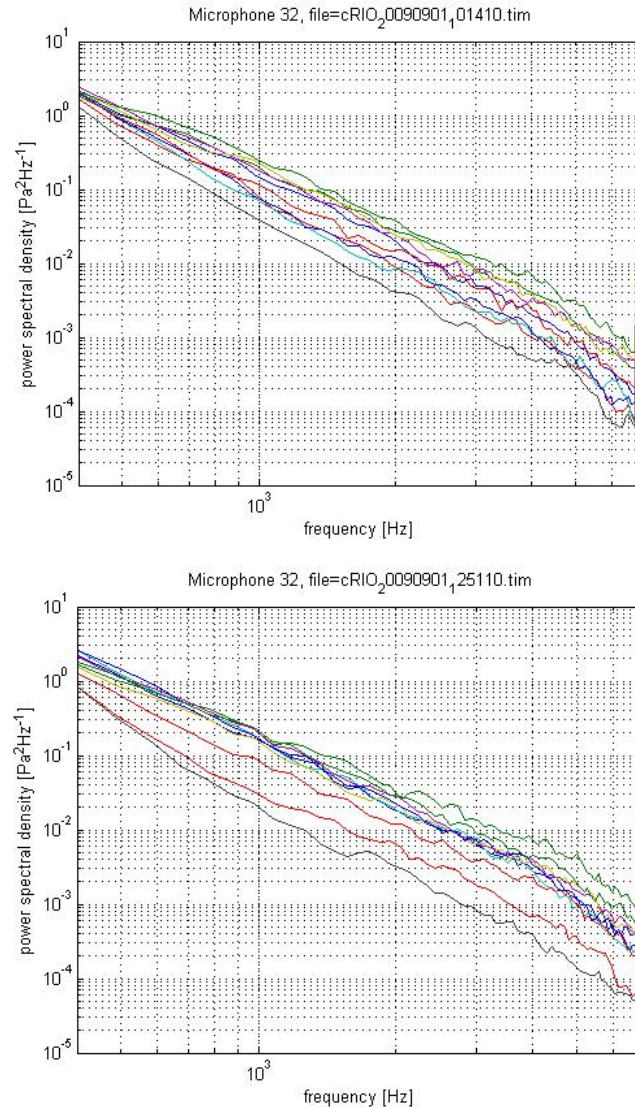

Figure 43 PSD spectra of signal from microphone 32 which is about 0.8 chord lengths from the leading edge for measurements on September 9 at 10:14 and 12:50 , respectively. Each line in the figures represents the spectrum of 1 sec. of the total time trace of 10 sec.

Spectra of the signal from microphone 32 which is situated about 0.8 chord lengths from the leading edge were derived for each 1 second block of the total length of 10 seconds. It is seen from Figure 43 that the spectra vary considerably from one period to the next and it is expected that variations in local inflow angle is the main cause. Therefore, the spectra will be correlated with the local inflow angle and it is expected that this will give a detailed picture of the trailing edge noise source.

6 Final remarks

The experiments conducted within the DAN-AERO MW project have briefly been described and a number of application examples of the experimental data have been presented. It is the hope that this will inspire readers of the present report to start using the data and perform much more detailed analysis of the data. As mentioned in the Preface section a new project has been funded by the Danish Energy Agency, EUDP, and a detailed analysis and utilization will be performed within this project.

It should also be noted that the data sets from the DAN-AERO MW project are not in general available for people outside the project group and the reporting on the project comprises a number of confidential, internal reports [11], [12], [13], [14]. However, specific requests on specific data sets will be evaluated by the project partners to assess the possibility of releasing the requested data sets.

7 References

[1] Johansen, J.; Sørensen, N.N., Airfoil characteristics from 3D CFD rotor computations. Wind Energy (2004) 7, 283-294.

[2] Madsen, H.Aa., "Aerodynamics of a horizontal-axis wind turbine in natural conditions". Risø-M-2903 (1991), 134 pp.

[3] Hand, M., Simms, D., Fingersh, L., Jager, D., Cotrell, J., Schreck, S., and Larwood, S., Unsteady Aerodynamics Experiment Phase VI: Wind Tunnel Test Configurations and Available Data Campaigns, NREL/TP-500-29955, December 2001. Available electronically at http://www.nrel.gov/docs/fy02osti/29955.pdf

[4] Schepers, J. G. and Snel, H.: 'Model Experiments in Controlled Conditions, Final report', ECN-E-07-042, Energy Research Center of the Netherlands, ECN, February 2007, http://www.ecn.nl/publicaties/default.aspx?nr=ECN-E--07-042

[5] Antoniou, I.; Jørgensen, H.E.; Mikkelsen, T.; Frandsen, S.; Barthelmie, R.J.; Perstrup, C.; Hurtig, M., "Offshore wind profile measurements from remote sensing instruments". In: Proceedings (online). 2006 European Wind Energy Conference and Exhibition, Athens (GR), 27 Feb - 2 Mar 2006. (European Wind Energy Association, Brussels, 2006) 10 p.

[6] Niels-Anker Olesen Vestas. Private communication

[7] Bak, C., Madsen, H. Aa., Paulsen, U. S., Gaunaa, M., Sørensen, N. N., Fuglsang, P., Romblad, J., Olesen, N. A., Enevoldsen, P., Laursen, J. Jensen, L. "DAN-AERO MW: Comparisons of airfoil characteristics for two airfoils tested in three different wind tunnels". Paper to be presented at the conference TORQUE2010 on Crete in June 2010.

[8] Madsen, H.Aa. and Fischer A. Wind Shear and Turbulence Characteristics from Inflow Measurements on the Rotating Blade of a Wind Turbine Rotor. In proceedings of EWEC2009 held in Marseille, France on March 16-19, 2009.

[9] Madsen, H. Aa., Bak, C., Paulsen, U. S., Gaunaa, M., Sørensen, N. N., Fuglsang, P., Romblad, J., Olesen, N. A., Enevoldsen, P., Laursen, J. Jensen, L. "The DAN-AERO MW Experiments". Paper AIAA 2010-645 presented at the 48th AIAA Aerospace Sciences Meeting Including the New Horizons Forum and Aerospace Exposition 4 - 7 January 2010, Orlando, Florida.

[10] Christian Bak, Helge Aa. Madsen,Uwe S. Paulsen, Mac Gaunaa, Niels N. Sørensen, Peter Fuglsang, Jonas Romblad, Niels A. Olsen, Peder Enevoldsen, Jesper Laursen, Leo Jensen, "DAN-AERO MW: Detailed aerodynamic measurements on a full scale MW wind turbine", Paper S3.3, EWEC 2010 conference, Warsaw, Poland, 20-23 April 2010

[11] Christian Bak, Helge Aa. Madsen, Mac Gaunaa, Witold Skrzypinski, Uwe Paulsen, Per Hansen, Michael Rasmussen, Peter Fuglsang, Niels A. Olesen, Jonas Romblad, Peder Enevoldsen, Jesper Laursen," DANAERO MW: Instrumentation of the NM80 wind turbine at Tjæreborg", Risø-I-3045(EN), Risø National Laboratory for Sustainable Energy Technical University of Denmark, Draft March 2010.

[12] Christian Bak, Helge Aa. Madsen, Mac Gaunaa, Uwe Paulsen, Per Hansen, Michael Rasmussen, Peter Fuglsang, Peder Enevoldsen, Jesper Laursen, Jonas Romblad, " DANAERO MW: Wind tunnel tests", Risø-I-3047(EN), Risø National Laboratory for Sustainable Energy Technical University of Denmark, Draft March 2010.

[13] Helge Aa. Madsen, Christian Bak, Uwe Schmidt Paulsen, Li Na, "DAN-AERO MW: Overview of inflow data on the Siemens 3.6 MW turbine at Høvsøre". Risø-I-3067 (EN), Draft April 2010.

[14] Christian Bak, Helge Aa. Madsen, Mac Gaunaa, Uwe Paulsen, Per Hansen, Michael Rasmussen, Niels A. Olesen, Jonas Romblad, Peter Fuglsang, Peder Enevoldsen, Jesper Laursen " DANAERO MW: Measurement campaigns on the NM80 wind turbine at Tjæreborg", Risø-I-3046(EN), Risø National Laboratory for Sustainable Energy Technical University of Denmark, Draft March 2010.

Risø DTU is the National Laboratory for Sustainable Energy. Our research focuses on development of energy technologies and systems with minimal effect on climate, and contributes to innovation, education and policy. Risø has large experimental facilities and interdisciplinary research environments, and includes the national centre for nuclear technologies.